

The Experimental Study of an SPWM-Based Controller in an Inverter

Muhammad Daniel Ahmad Kamal¹, Jabbar Al-Fattah^{1*}

¹ Department of Electrical Engineering, Faculty of Electrical and Electronic Engineering, Universiti Tun Hussein Onn Malaysia, 86400 Parit Raja, Johor, MALAYSIA

*Corresponding Author: jabbar@uthm.edu.my

DOI: <https://doi.org/10.30880/eeee.2025.06.02.054>

Article Info

Received: 24 January 2025

Accepted: 22 May 2025

Available online: 30 October 2025

Keywords

SPWM-Based Controller, Single-Phase Inverter, Total Harmonic Distortion, and LC Filter.

Abstract

This project tends to design and implement an SPWM inverter to provide a stable AC output with low THD value according to IEEE 1547 standards for applications in solar power systems. MATLAB/Simulink checks the efficiency at different loads and frequencies and incorporates a modified MPPT charge controller for a stable input. This chapter presents the design and application of a solar power system with an AC source for a load. This isotype needs a solar panel, boost converter, MPPT charger, and Arduino operated SPWM inverter/LC filter/MCCB in it. Tasks include system design, MATLAB Simulink, integration of hardware components, and cobbling up of the system in C-code, with strong consideration of feedback control, debugging, and confirmation of the system. This project proposes and implements the design, simulation, and realization of a solar-powered SPWM inverter intended for AC loads. MATLAB Simulink was used to ensure proper characterization of design parameters, best waveform quality, and reduced THD. As tested, the hardware output was stable at different frequencies and voltages, following the specified IEEE standards and offering reliable performance for clean sinusoidal AC power production. Constructed using the SPWM technique, this solar inverter project generated a clean, stable AC with a low THD, as confirmed by MATLAB Simulink and the actual hardware. Under conditions of variable load and frequency, in compliance with IEEE 1547 standards, the system was effective, stable, and capable of small-scale renewable energy applications and supply of single-phase AC loads such as household appliances.

1. Introduction

An inverter is an essential component of solar energy systems because it takes DC electricity produced by solar panels and changes it into the AC electricity that most home appliances and utility companies use. The two forms of an inverter are sinusoidal pulse width modulation inverter (SPWM inverter) and sine wave inverter (normal inverter) which two differences in many factors including efficiency and quality of the waveform output. A sinusoidal pulse width modulation (SPWM) inverter is a power electronic converter that converts the DC supply to AC output. The SPWM or bandwidth is determined by two chief parameters which are Modulation Index and Modulation Frequency. The SPWM inverter finds its application in power systems, motor control, and renewable energy systems, especially for the generation of high-quality sinusoidal AC [1]. Through SPWM modulation, the waveform output by the inverter is a sinusoidal one whereas minimizing the THD and dv/dt

compared to a normal inverter that directly switches the supplied DC supply voltage between maximum and zero voltages producing a non-sinusoidal output waveform. Since the sinusoidal output of the SPWM inverter reduces the current distortion, it improves motor efficiency, and reduces the voltage stress, which is a major cause of motor breakdown, the SPWM inverter is more suitable for motor drives. Though the standard inverter is widely used, for motor drive applications, the SPWM inverter is found to be more reliable and efficient [2]. To determine the actual characteristics of the inverter, several tests for it are performed using both the purely resistive and the inductive loads. The inductive load produces magnetic fields and changes current into mechanical energy. Other types of load do not produce magnetic fields and convert the current into heat known as the resistive load. The capability of the inverter to give sinusoidal output voltage together with low THD assures proper power delivery with minimized threat of harmonic distortion that may harm and complicate apparatuses [3]. The problem that comes with this project is to analyze the energy efficiency of a Sinusoidal Pulse Width Modulation (SPWM) based controller in an inverter for solar which has stable and good Alternating Current (AC) voltage output, power, and Total Harmonics Distortion (THD) as per the standard as required by the IEEE 1547. Next, the other crucial challenge is to make the inverters should be stable and perform well to suit their intended application inverter and their performance under the diverse load and frequency range. However, it is difficult to sustain steady stabilities and achieve the best performances because of some conditions such as switching dynamics, and harmonics distortions among other load conditions. New challenges have arisen as regards system frequency stability. In addition, IESS is utilized as a frequency stability compensator since inverter-interfaced energy storage systems manage to mitigate such deterioration by responding quickly and effectively [4].

2. Literature Review

2.1 SPWM-Based Controllers

The FA PI (Proportional-Integral) controller is used by the SPWM (Sinusoidal Pulse Width Modulation) based controller to control the modulation index of the SPWM signals that drive the IGBT gates. Particle Swarm Optimization (PSO) is used to optimize the PI controller to reduce error and enhance waveform quality. Even in the presence of faults or imbalanced load situations, the PI controller maintains a steady output voltage and current waveform by modifying the modulation index in response to the load voltage feedback [5]. The control system applies a transformation process to acknowledge the three-phase AC signals as a single rotating reference frame that achieves easy control and analysis of the supplied signals. These control signals are then converted back from the three-phase system where modulating signals are produced and then utilized in the SPWM process for controlling the VSI switches [6].

2.2 Single-Phase Full Bridge Inverter design

Single phase full-bridge inverter as shown in Fig. 1 is an electronic device used under the category of power electronics to convert direct current (DC) power into alternating current power. The processor of the microprocessor 5V consists of four switches applied in full-bridge topology and it employs the same pulse width modulation signal to produce the output of a square waveform [7]. Moreover, an improved voltage controller for the inverter is designed by developing a cascade fractional-order PID (FO-PID) controller using the fundamentals of the conventional FO-PID controller [8]. The system is expanded to regulate various types of loads and can operate at varied modes relative to the resistive and inductive loads.

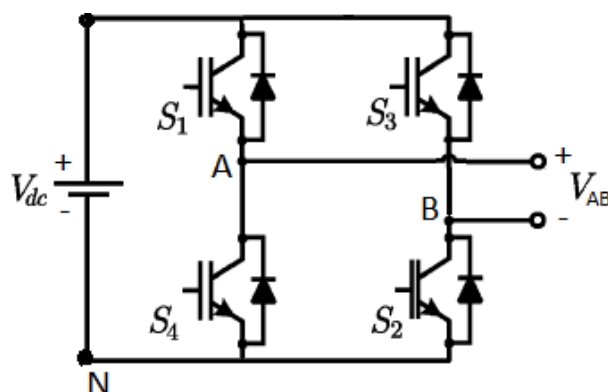


Fig. 1 Single-Phase Full-Bridge Inverter Circuit

2.3 Harmonic Filter (LC Filter)

An LC harmonic filter as shown in Fig. 2 is simply an electrical gadget put in a circuit to eliminate tiny harmonic particles as well as assist in canceling out reactive power. These are the inductors (L) and capacitors (C) that are resonant to operate on preselected harmonics of the supply system voltage. This means that LC filters help to minimize these challenges, at the same time improving the value of the power factor of the system [8]. The specific use of passive Power Harmonic Filter (PHF) is to improve the quality of power by compensating photon reactive power and restricting volt and current harmonics in a power system. Regarding the operation of the PHF, it is expected to be designed in a way that the filter equivalent impedance of the harmonic to be eliminated would always be less than the grid equivalent impedance of this harmonic to achieve the best results and enhance the efficiency of this grid filter. It is the topological and parametric design of the PHF where the improvements in the efficiency of harmonic suppression are mostly prominent. For instance, preserving a particular topology of a passive power harmonic filter (PHF) and the control parameters for appropriate filtering of harmonics while not impacting other power quality issues [9].

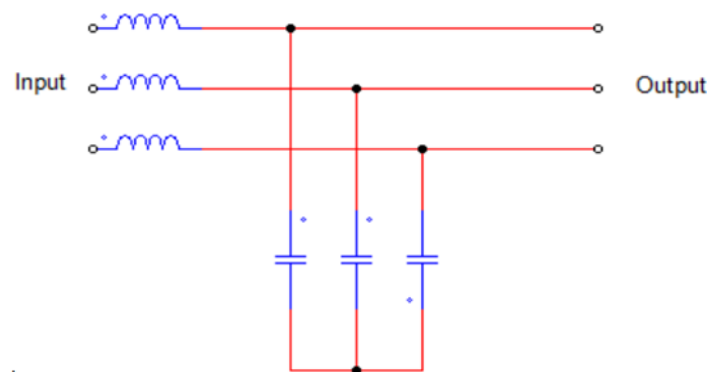


Fig. 2 LC Filter Circuit

3. Methodology

This section explains and depicts the techniques and procedures used throughout the project's conception and development. The method's description should be more detailed before it is implemented. Therefore, this section will be used to review the project's block diagram, title, problem definition, and software and hardware choices.

3.1 Proposed Design

Fig. 3 shows the overall view of the solar power system to provide AC power to the load like a lamp. The first component is a solar panel that directly converts sunlight into DC electricity supplied to the isolator for safety from the backflow of electricity. The DC power obtained is then passed through a boost converter with the specific voltage being regulated using an Arduino Uno microcontroller and an L298N gate driver for the boost converter. Subsequently, the obtained increased DC voltage is converted to AC by a single-phase inverter. When out of the inverter, an LC filter smooths the output in case there are any ripples in the AC voltage. As for this AC power, it gets through a Molded Case Circuit Breaker (MCCB) that serves as the means of circuit protection. Lastly, it arrives at the AC load which can be a lamp. The MPPT charger is meant to do the charging of a battery which is another component that stores energy in the form of electrical charge. There is another switch that is connected to another Arduino Uno and Totem-Pole Gate Driver this switch controls the flow of power from the battery to the system. In this way when there is not enough power supplied from solar it will automatically turn on the battery to supply power to the load and ensure continuous power supply to it.

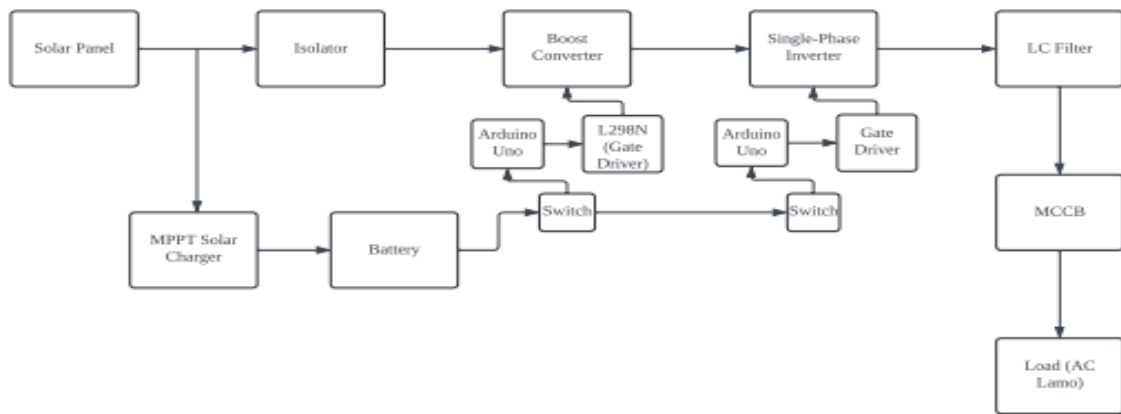


Fig. 3 Block Diagram for The Project

3.2 The Complete System

Fig. 4 illustrates the step-by-step process for designing and integrating a solar power system. It begins with stating design specifications, followed by mathematical calculations to determine component specifications, including solar panels, batteries, and SPWM inverters. A circuit diagram is created in MATLAB to visualize component relationships, and adjustments are made if specifications are not met. Once finalized, components are procured and integrated into the hardware architecture. The SPWM inverter code is programmed, tested, and uploaded to an Arduino Uno, with troubleshooting as needed. Each component is individually tested before assembling the system, which is installed at Jalan Lestari, UTHM. Final system connections and coding are aligned, and operational data is collected to evaluate the system's efficiency and effectiveness, concluding the process.

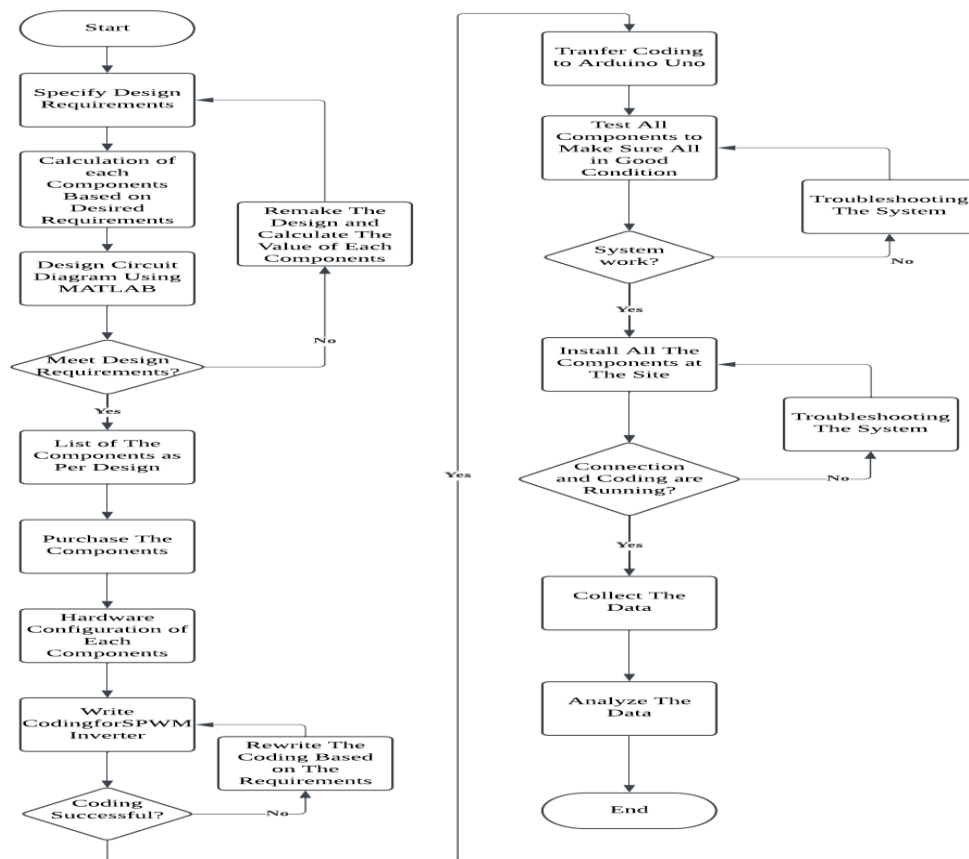


Fig. 4 Overall implementation of the study

3.3 Single-Phase Full-Bridge Inverter

The inverter of this project is a single phase that is placed on a PCB board following type of MOSFETs are used four MOSFETs with heat sinks to manage thermal load as shown in Fig. 5. The parts used for the single-phase inverter are given below in Table 3.1 the diagram of hardware implementation is represented here since the main horsepower of the digital signal processing is delivered from the microcontroller, which is the real heart of the system, and the hierarchy of the system is decentralized for better control and flexibility.

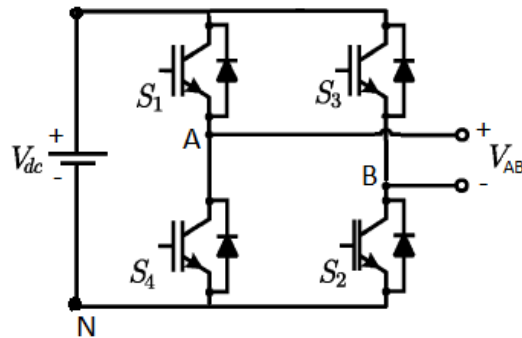


Fig. 5 Single-Phase Full-Bridge Inverter Circuit

Table 1 List of Components.

No.	Components	Detail	Quantity
1	MOSFET	IRFP460	4
3	Heat Sink	medium	4
4	PCB Board	Single-Phase Full-Bridge InverterDesign	1

3.4 Gate Driver Connection

The gate driver circuit converts PWM signals into control signals required for inverter switches as shown in Fig. 6. Hence, for this project, the L298N gate driver is used to modulate PWM signals. More importantly, it acts as a safety measure for the inverter switches. Due to the dual PWM signal requirements, the gate driver is set to drive gates S1, and S4 of the circuit for one signal and gates S2 and S3 for the other. This way, it is possible to avoid wear outs and prevent the burnouts of the inverter switches.

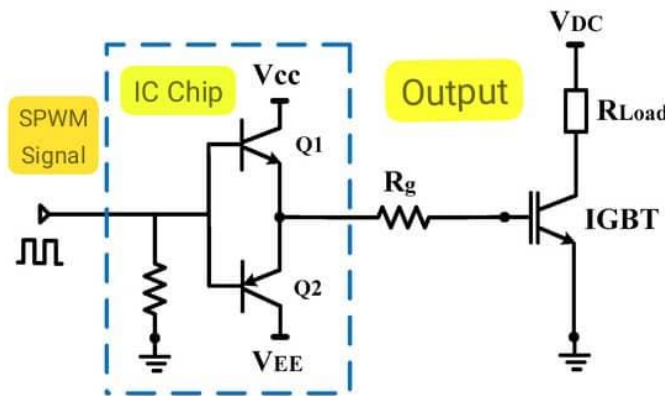


Fig. 6 Totem-Pole Gate Driver Pinouts

3.5 LC Filter Circuit

This LC filter circuit as shown in Fig. 7 is commonly applied to realize low pass filtering of high-frequency signals, 20kHz SPWM waveform output into a continuous low-frequency waveform. It is comprised of a 15µF capacitor and a 10mH inductor. While the capacitor supplies or absorbs the energy to even out fluctuations in voltage, the inductor opposes fast changes in current. They work well to eliminate the fundamental frequency at 50Hz from the switching noise by eliminating the high-frequency PWM components. This procedure minimizes the harmonic distortion and brings stability in the sense that none of the output waveforms varies significantly from a standard sinusoidal 50Hz AC source. The capacitor is calculated from the given equation (1) to (3).

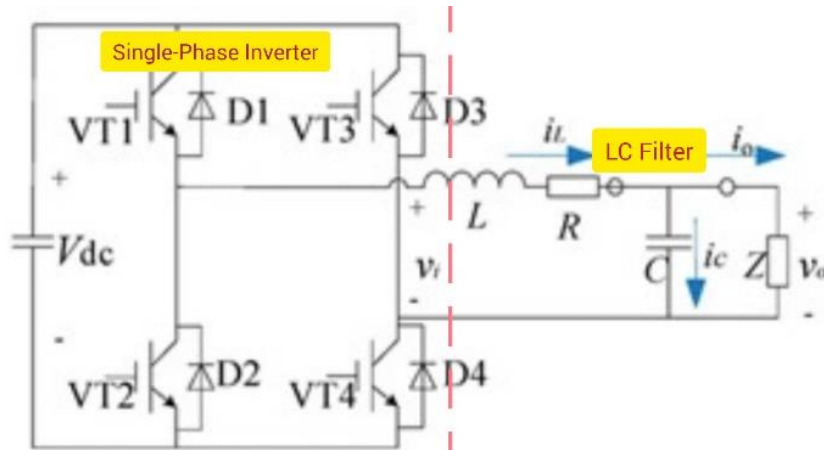


Fig. 7 LC Filter Circuit

$$f_c = \frac{1}{2\pi\sqrt{LC}} \quad (1)$$

$$C = \frac{1}{((2\pi \times 411)^2(10 \times 10^{-3}))} \quad (2)$$

$$C = 15 \mu F \quad (3)$$

4. Result and Analysis

The conclusions of this work and the results achieved in the further simulation and hardware implementation stage will be considered in this section. For checking the validity of the employed calculation for the components, the MATLAB Simulink simulations are used to know the extent of their conformity with the requirements before actually constructing the hardware setup. Then, the coding for controlling the capability of output frequency and voltage is sent and the Arduino uno with single phase inverter tests the AC lamp system, The AC lamp performance of the controller, the precise degree of SPWM signal, and the general stability and energy-saving factor of the ac lamp, these aspects and questions are the major issues focuses on. The used control methods are compared with the simulation and actual results of the model in other to approve a hypothesis. The last part of the section involves the discussion of various implications of the results.

4.1 Logic Gate System Output Signal

MATLAB Simulink is used to test a single-phase full-bridge SPWM inverter to ensure that the values calculated by the components meet the desired specifications before implementing a hardware wiring. In Simulink, a precise working of the single-phase full-bridge inverter is developed wherein the SPWM technique is used for creating the correct gate signals of the inverting switches. Fig. 8 is a plot of a waveform with a triangular in the shape of the letter A, ranging from -1 to 1, the second graph with a waveform at 0 and 1 related to a square waveform during positive cycles which is an output signal from S1 and S3. At the bottom is also a square waveform but during negative cycles which is an output signal from S2 and S4. This means the time in microseconds, which is presented on the x-axis indicating higher frequency signals. Some of the possible applications of the triangular waveform may have been with a SPWM strategy and the two square waves may have meant SPWM outputs. This leads to the conclusion that the display illustrates how the modulating triangular wave generates the square waves shown displayed, ideal in control systems or signal processing to indicate the duty cycle.

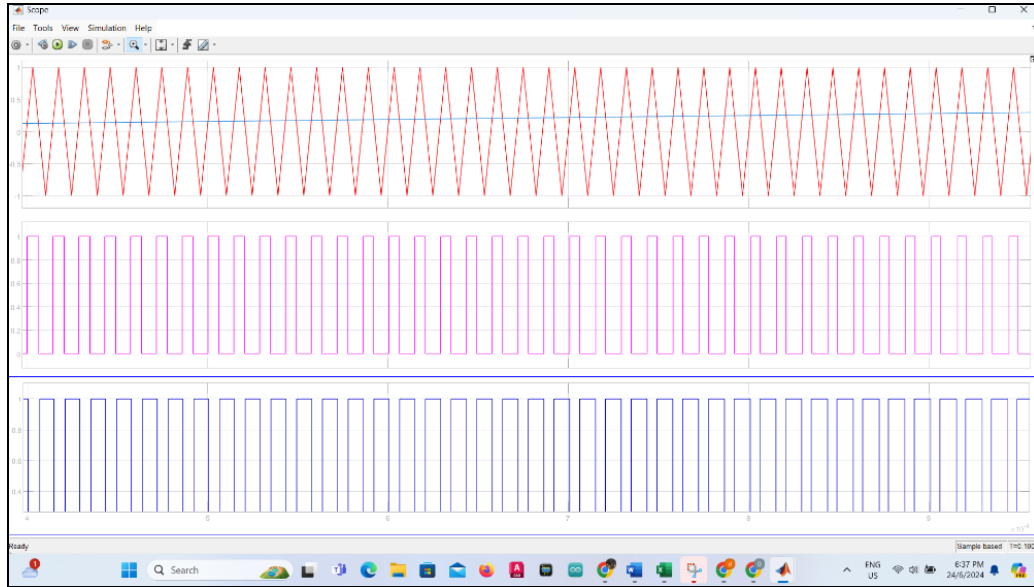


Fig. 8 Logic gate System Output

4.2 AC Output Signal from LC Filter

Fig. 9 shows two plot results of a simulation provided where the red curve is of the voltage output and the blue curve is of the current output. Therefore, it should be noted that in the case of the examined waveform, the red voltage waveform, the peak-to-peak value equals 90.14V and the blue current waveform's peak-to-peak value is 0.901 A. The input supplied to this system includes a 45V DC voltage signal. The waveform evidence suggests that it may be an inverter-kind of circuit transforming the direct current input to the alternating current output and that is why the voltage, and the current are sinusoidal.

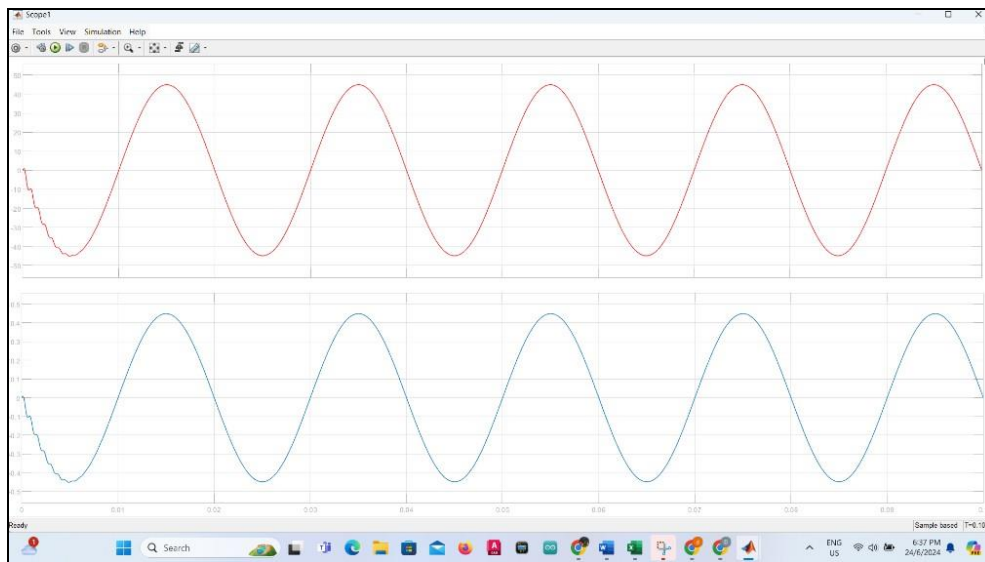
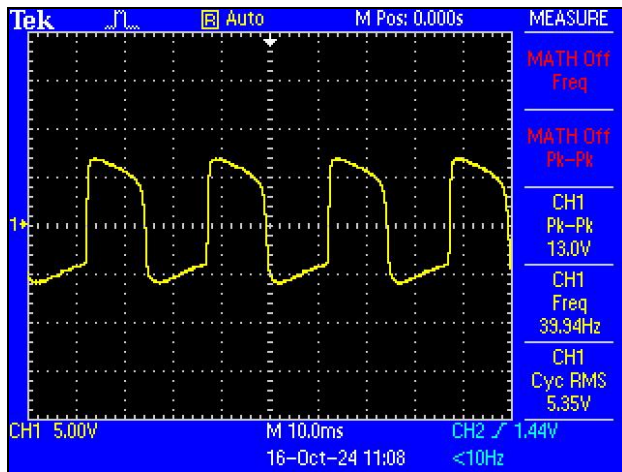


Fig. 9 Voltage and Current Output

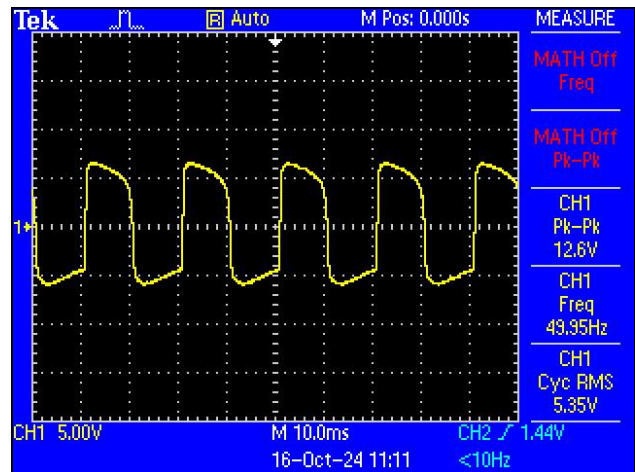
4.3 SPWM Output Signal with Different Frequency Setting (40Hz, 50Hz, 60Hz)

Fig. 10 (a), (b) and (c) shows results obtained from a system designed to be used under an input voltage of 5.0V using three frequencies. At the frequency of 39.94 Hz, the ripple voltage is 0V and the output voltage is 13.0V, then the system generates output more than input. At 49.95 Hz, the output voltage was slightly lower, and the stabilized value was 12.6V this can be attributed to a certain inefficiency or power conversion in the output. As the frequency of the signal increases in the case of 59.94 Hz the output voltage is reduced to 12.2V and the same trend is seen by progressive reducing the voltage with the increasing frequency. Stating simply, the conversion of output voltage takes place according to the frequency of the input voltage. A higher frequency results in a

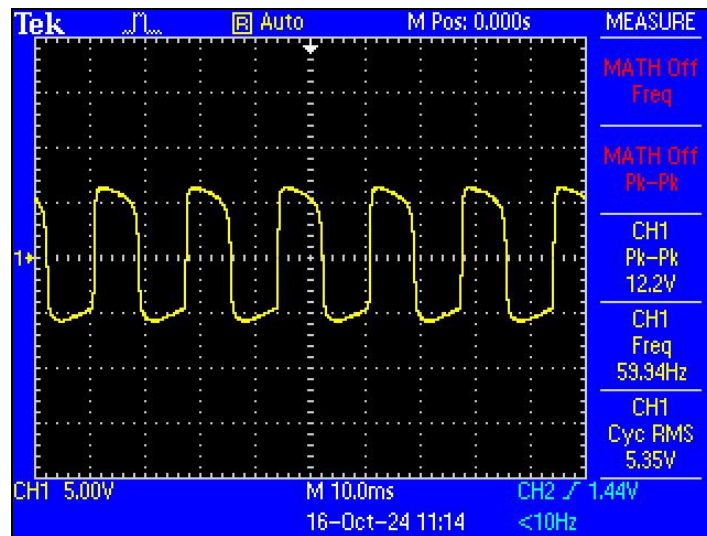
slightly lower output voltage as can be attributed to design or limitations on the available circuit components. Table 2 is tabulated the results of comparison of differences setting of switching frequency (40Hz, 50Hz, 60Hz).



(a) An Arduino Uno SPWM Output Signal (40Hz)



(b) An Arduino Uno SPWM Output Signal (50Hz)



(c) An Arduino Uno SPWM Output Signal (60Hz)

Fig. 10 Results of An Arduino Uno SPWM with various frequency

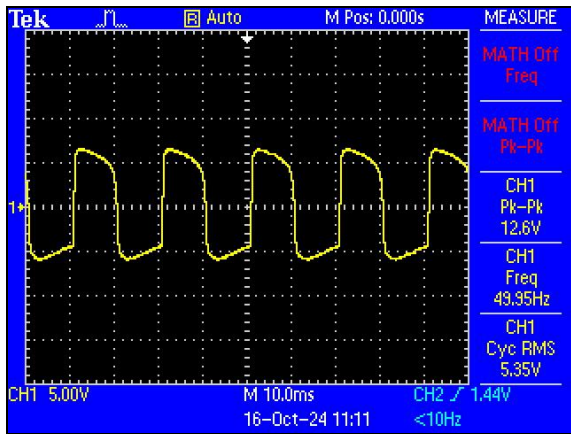
Table 2 Comparison of Differences Setting of Switching Frequency (40Hz, 50Hz, 60Hz)

Input Vdc (V)	Frequency (Hz)	Output Vac (V)	RMS Voltage (V)
5.0	39.94	13.0	5.35
5.0	49.95	12.6	5.13
5.0	59.94	12.2	4.87

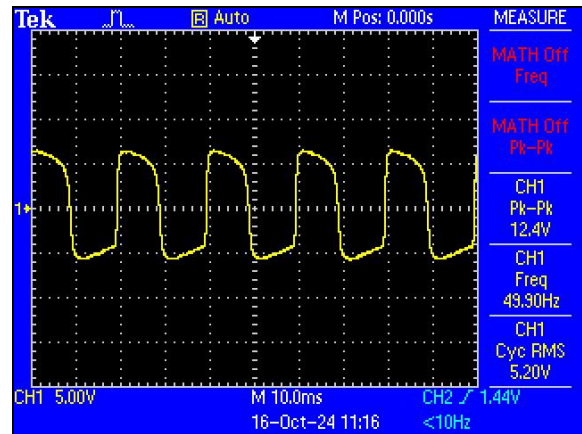
4.4 SPWM Output Signal (50Hz) with Different Output Voltage Setting (100%, 80%, 50%)

Fig. 11 (a), (b) and (c) shows the output signal with different output voltage settings. While Table 3 tabulated the results of the performance of a system with an input DC voltage of 5.0V as the input utilization, focusing on using the output parameters such as RMS voltage, frequency, and output DC voltage. They are as follows, with an initial RMS voltage of about 5.35 V, the RMS voltage reduces to about 5.20 V and further to about 4.88 V showing little fluctuation in the effective value of the AC waveform over or under conditions. Likewise, the system's output voltage changes gradually from 12.6 V to 12.4 V and further to 11.6 V, which suggests a slight variation in

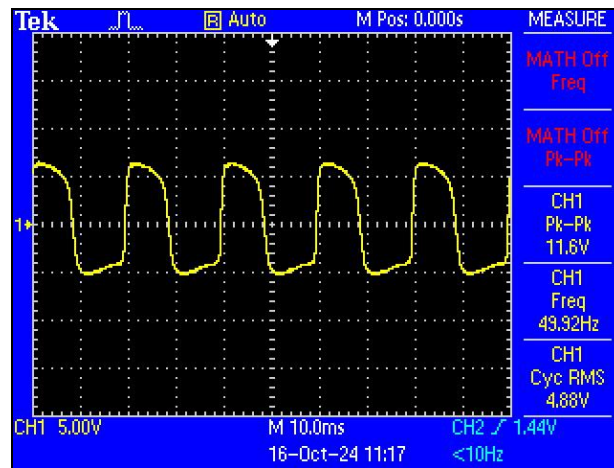
the efficiency of the circuit, or the load partnered with it. The frequency is kept constant at 49.95 Hz in all measurements which implies that the signal oscillation frequency does not change with these voltage alterations. Overall, the data has captured how the system moves or reacts to any changes in the input values, and how it continues to operate at fixed frequencies and produce comparatively set output levels.



(a) Arduino Uno SPWM Output Signal (100%)



(b) Arduino Uno SPWM Output Signal (80%)



(c) Arduino Uno SPWM Output Signal (50%)

Fig. 11 Results of different output voltage setting

Table 3 Comparison of Differences Setting on Output Voltages (100%, 80%, 50%)

Output (%)	Input Vdc (V)	RMS Voltage (V)	Frequency (Hz)	Output Vdc (V)
100	5.0	5.35	49.95	12.6
80	5.0	5.20	49.95	12.4
50	5.0	4.88	49.95	11.6

4.5 Total Harmonic Distortion (THD) Analysis

The spectrum in Fig. 12 displays a signal with a fundamental frequency at 50 Hz, indicated by Cursor 1 with a magnitude of 13.8 dB. Another notable harmonic is observed at 150 Hz (Cursor 2) with a magnitude of 3.01 dB, representing the third harmonic. The graph also reveals the presence of additional higher-order harmonics at decreasing dB levels.

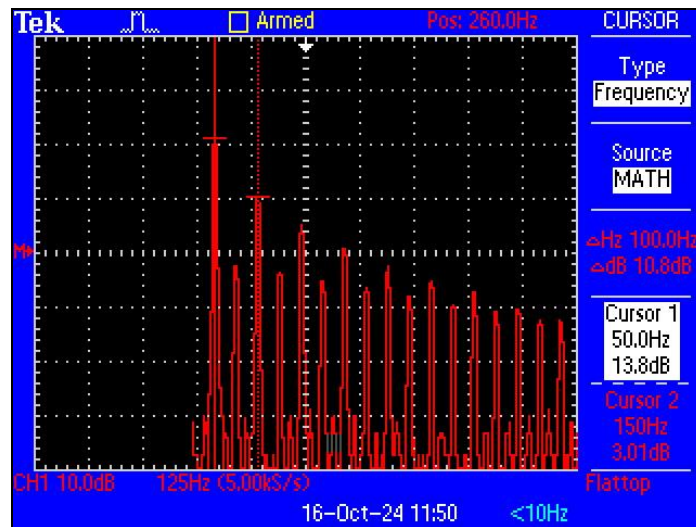


Fig. 12 THD comparison between 50Hz (Fundamental Frequency) and 150 Hz.

The spectrum in Fig. 13 displays a signal with a fundamental frequency at 50 Hz, indicated by Cursor 1 with a magnitude of 13.8 dB. Another notable harmonic is observed at 885 Hz (Cursor 2) with a magnitude of -47 dB, representing the third harmonic. The graph also reveals the presence of additional higher-order harmonics at decreasing dB levels.

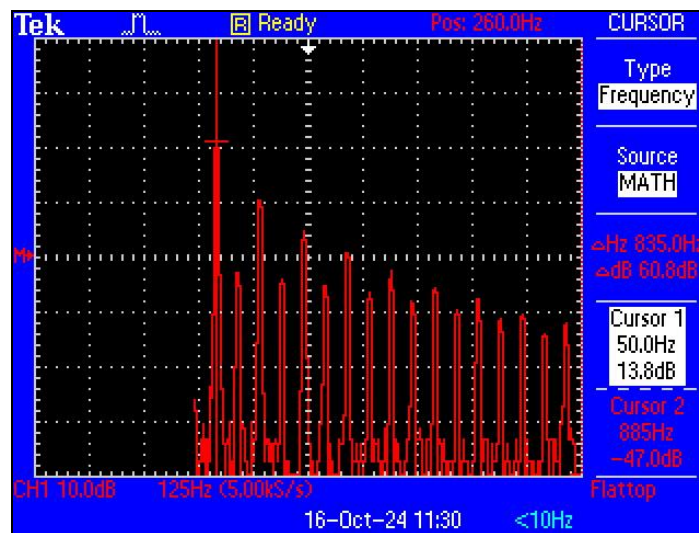


Fig. 13 THD comparison between 50Hz (Fundamental Frequency) and 885Hz

The spectrum analysis reveals that the system operates at a base frequency of 50 Hz with a magnitude of 13.8 dB, representing its primary operating frequency. A harmonic at 150 Hz with a lower magnitude of 3.01 dB indicates minimal signal distortion, likely due to system instabilities or nonlinear circuit behaviour. In another case, this harmonic shifts to 885 Hz with a much lower magnitude of -47.0 dB, showing effective attenuation of higher harmonics. Table 4 tabulated a harmonic frequency beyond the tertiary range have negligible magnitudes, highlighting the system's ability to dampen higher-frequency noise and maintain the dominance of the fundamental frequency.

Table 4 Table of THD Analysis

Figures	Fundamental Frequency (Hz) / Cursor 1	Magnitude of Cursor 1 (dB)	Frequency (Hz) / Cursor 2	Magnitude of Cursor 2 (dB)
12	50	13.8	150	3.01
13	50	13.8	885	-47.0

5. Conclusion

This project successfully developed and tested an SPWM inverter for solar-generated power, delivering steady AC voltage with reduced THD. Six solar panels were configured in a series-parallel arrangement to enhance power output and ensure stability under varying sunlight conditions. System design began with MATLAB Simulink simulations to optimize the SPWM control algorithm, LC filter parameters, and inverter switching performance for efficient AC waveform generation. Hardware development included solar panel assembly, an MPPT charger for optimal power extraction, a boost converter for voltage regulation, and an Arduino Uno-based inverter supported by a totem pole gate driver. Experimental tests at various frequencies (40 Hz, 50 Hz, 60 Hz) and power levels confirmed the system's stability, reliability, and compliance with IEEE standards, with low THD and effective harmonic elimination. The inverter powered household appliances efficiently, demonstrating its practicality for small-scale renewable energy systems. Future improvements could include advanced MPPT algorithms, enhanced cooling, and support for three-phase loads.

Acknowledgement

The authors would also like to thank the Faculty of Electrical and Electronic Engineering, Universiti Tun Hussein Onn Malaysia for its support.

Conflict of Interest

Authors declare that there is no conflict of interest regarding the publication of the paper.

Author Contribution

*The authors confirm contribution to the paper as follows: **study conception and design:** Muhammad Daniel Ahmad Kamal, Jabbar Al-Fattah; **data collection:** Muhammad Daniel Ahmad Kamal; **analysis and interpretation of results:** Muhammad Daniel Ahmad Kamal, Jabbar Al-Fattah; **draft manuscript preparation:** Muhammad Daniel Ahmad Kamal, Jabbar Al-Fattah. All authors reviewed the results and approved the final version of the manuscript.*

References

- [1] Abdolrasol, Maher G. M., et al. "Optimal PI Controller Based PSO Optimization for PV Inverter Using SPWM Techniques." *Energy Reports*, vol. 8, Apr. 2022, pp. 1003–11, <https://doi.org/10.1016/j.egy.2021.11.180>. Accessed 6 June 2024.
- [2] Abdulazeez Alsalemi and Ahmed M. Massoud. "Effortless Totem-Pole Converter Control Using a Power Factor Correction Peak Current-Mode Controller." *Sensors (Basel, Switzerland)*, 24 (2024). <https://doi.org/10.3390/s24154910>.
- [3] Abdulrahman and G. Radman, "Simulink-Based Program for Simulating Multi- Machine Power Systems," 2018 IEEE Power & Energy Society General Meeting (PESGM), Portland, OR, USA, 2018, pp. 1-5, doi: 10.1109/PESGM.2018.8585773.
- [4] Ahsan, M. Z., et al. "Performance Analysis of Unipolar SPWM Inverter: Resistive Load and Inductive Load." *IOP Conference Series*, vol. 932, no. 1, Sept. 2020, pp. 012074–74, <https://doi.org/10.1088/1757-899x/932/1/012074>. Accessed 15 Nov. 2023.
- [5] H. Kareem and D. Dunaev, "The Working Principles of ESP32 and Analytical Comparison of using Low-Cost Microcontroller Modules in Embedded System Design," 2021 4th International Conference on Circuits, Systems and Simulation (ICCS), Kuala Lumpur, Malaysia, 2021, pp. 130-135, doi: 10.1109/ICCS51193.2021.9464217.
- [6] Noorsal, E.; Rongi, A.; Ibrahim, I.R.; Darus, R.; Kho, D.; Setumin, S. Design of FPGA-Based SHE and SPWM Digital Switching Controllers for 21-Level Cascaded H-Bridge Multilevel Inverter Model. *Micromachines* 2022, 13, 179. <https://doi.org/10.3390/mi13020179>
- [7] Rohmad Praditya Alma'a and Ir. Bana Handaga. "Power Amplifier Kelas D Self Oscillating Dengan Power Mosfet Irfp4227, Irfp250n Dan Irfp460." (2017).
- [8] Noorsal, E.; Rongi, A.; Ibrahim, I.R.; Darus, R.; Kho, D.; Setumin, S. Design of FPGA-Based SHE and SPWM Digital Switching Controllers for 21-Level Cascaded H-Bridge Multilevel Inverter Model. *Micromachines* 2022, 13, 179. <https://doi.org/10.3390/mi13020179>
- [9] Geddada, Nagesh, et al. "Synchronous Reference Frame Based Current Controller with SPWM Switching Strategy for DSTATCOM Applications." *2012 IEEE International Conference on Power Electronics, Drives and Energy Systems (PEDES)*, Dec. 2012, <https://doi.org/10.1109/pedes.2012.6484393>. Accessed 23 June 2024.